

## P7-12

# Amorphous Silicon/Silicon-Carbide Separated Absorption and Multiplication Region Avalanche Photodiode with Additional Doped Superlattice

Neng-Fu Shih, Wen-Jung Chuang<sup>1</sup>, Jyh-Wong Hong<sup>1</sup>

Department of Electrical Engineering, Hsiuping Institute of Technology

No.11, Gungye Rd., Dali, Taichung, 412, Taiwan, R. O. C.

Phone No.:886-4-24961369 E-mail: nfshih@ieee.org,

<sup>1</sup> Department of Electrical Engineering, National Central University, Chungli 32054, Taiwan, R. O. C.

Phone No.:886-3-4227151 ext. 4477

## 1. INTRODUCTION

Low noise operation at high gain is a desirable requirement for photodetectors in optical communication systems. Photomultiplier tube is the photodetector with highest gain at lowest noise of any existing photodetector. However, its large size, high-voltage requirements, and after pulsing [1] limits its usefulness.

Avalanche photodiodes (APD's) provide gain through carrier multiplication in semiconductor materials, alternately. Especially, APD's are used widely as detectors in fiber-optic communication systems. The potential advantages of APD's as detectors for optical communication systems have been well established [2].

Low excess noise can be obtained in an avalanche photodiode when the electron and hole impact ionization differs greatly as demonstrated by McIntyre [2]. Much interest has been generated in "artificial" enhancement of the electron to hole ionization rate ratio through use of superlattice device structures [5-6] due to most III-V semiconductors have nearly equal electron and hole ionization coefficients [3,4]. These structures make use of the band edge discontinuity at a heterostructure interface to produce a large increase in the electron ionization rate. The electron ionization rate can be substantially large than the hole ionization rate provided that the conduction band edge discontinuity is much larger than the valance band edge difference.

Several general methods have recently been developed by artificially enhancing the electron to hole ionization rates ratio through selective heating of the electron distribution. In all of these devices, the electron ionization rate is greatly enhanced over the hole ionization rate and is also made more spatially deterministic than in conventional APD's [6].

## 2. THEORY AND DEVICE OPERATION

The structure and energy-band diagrams under reverse-bias of an amorphous SAM-DSAPD are illustrated in Fig. 1 and Fig. 2 respectively. The device consisted of alternating layers of a-Si and a-SiC. When an electron enters the narrow bandgap material, a-Si, from the wider bandgap material, a-SiC, its kinetic energy is increased by the conduction band offset  $\Delta E_c$ . The electron essentially "sees" a reduced ionization threshold energy.

Since the impact ionization rate depends exponentially upon the threshold energy, the electron can more readily impact ionize. Therefore, if  $\Delta E_c$  is substantially larger than  $\Delta E_v$ , it is expected that the electron ionization rate would be much larger than the hole ionization rate.

## 3. FABRICATION PROCESS

We use an ITO-coated Corning 7059 glass plate as the substrate. After cleaning process, the substrate was put into a PECVD system to deposit various amorphous films on the substrate, as shown in Fig.1. Right hand side in fig.1 shows the flow rate of process gas. Then the Al electrodes (250 nm) were deposited on the top n<sup>+</sup>-a-Si:H layer to serve as an ohmic electrode through the use of an E-beam coater. The diameter of the electrode defined by the circular metal mask was 1.2 mm, i.e., the device area was  $1.13 \times 10^{-2} \text{ cm}^2$ .

The sample was put into a rapid thermal annealing (RTA) system. The RTA chamber was filled with H<sub>2</sub> and kept at 1 atm. The raising rate of temperature was set to be 10 °C/s, then, the temperature was maintained at 300 °C for 10 minutes. Finally, the chamber was cooled down to room temperature naturally. With an annealing process, not only a better ohmic contact between the amorphous layer and external electrode would be obtained, but also the quality of the amorphous films became better since the hydrogen atoms might be attached to the dangling bonds in amorphous films.

## 4. Experimental Results

Fig. 3 gives the dark current and the photo-current with the incident power of 10 mW at a incident wavelength of 0.45 μm under vary biased condition, where open circles indicate photo-current and filled squares indicate the dark current, respectively. The variation of the photo-current for the applied voltage smaller than 12V and the dark current for the applied voltage smaller than 14 V could be due to the trapping and de-trapping effect of the trapping center in a-Si:H and a-SiC:H material.

Fig. 3 also presents the optical gain vs. applied voltage for the proposed SAM-DSAPD. As the applied voltage > 12 V, the optical gain starts to exceed 1, where the optical G is defined as

$$G = (I_{ph}/q)/(P_{in}/h\nu),$$

where the  $I_{ph}$  indicates the photo-current,  $q$  carrier charge,  $P_{in}$  incident power,  $h$  plank constant, and  $\nu$  incident wavelength, respectively. Optical gain higher than 1 is primarily due to the impact ionization process described previously. A maximum optical gain of 231 can be obtained when the applied voltage = 35 V.

## 5. CONCLUSIONS

The amorphous SAM-SAPD with additional p-i(a-SiC)-i-n(a-Si) layers in the substage of superlattice multiplication region had the higher optical gain, which would generate a higher output current when the devices were operated near the breakdown voltage. Using a higher electric-field and/or energy-band edge discontinuity in the multiplication region would improve the performance of an APD.

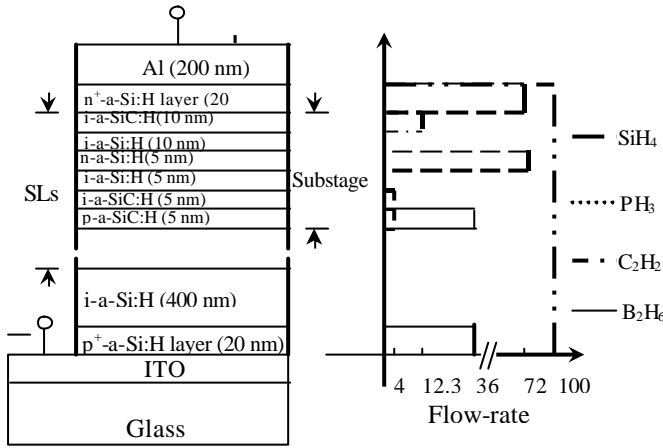


Fig. 1 the schematic cross-section along with the gas flow-rates for the amorphous SAM-DSAPD with additional p-i a-SiC:H i-n a-Si:H layers in a substage of superlattice (3 stages as given).

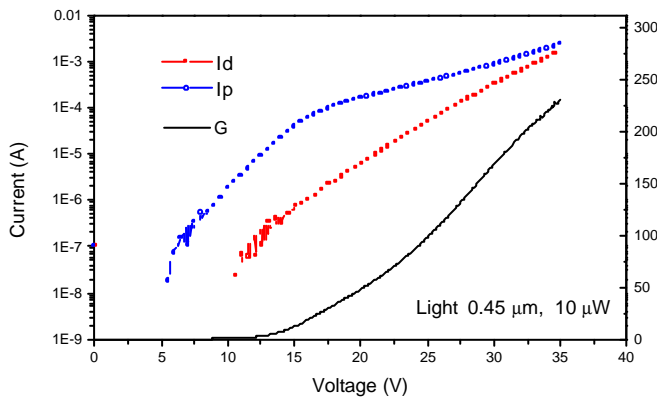


Fig. 3 the dark current, the photo-current, and the optical gain with the incident power of  $10 \mu\text{W}$  at a incident wavelength of  $0.45 \mu\text{m}$  under vary biased condition, where open circles indicate photo-current, filled squares indicate the dark current, and the solid line indicates the optical gain, respectively.

## REFERENCES

- [1] M. C. Teich, K. Matsuo, and B. E. A. Saleh, "Counting distributions and error probabilities for optical receivers incorporating superlattice avalanche photodiodes," IEEE Trans. Electron devices, vol. ED-33, pp. 1475-1488, 1986.
- [2] R. J. McIntyre, "Multiplication noise in uniform avalanche diodes," IEEE Trans. Electron Devices, vol. ED-13, pp. 164-168, 1966.
- [3] G. E. Bulman, V. M. Robbins, K. F. Brennan, K. Hess, and G. E. Stillman, "Experimental determination of impact ionization coefficients in (100) GaAs," IEEE Electron Device Lett., vol. EDL-4, pp. 181-185, 1983.
- [4] K. Brennan, "Theory of electron and hole impact ionization in quantum well and staircase superlattice avalanche photodiode structures," IEEE Trans. Electron Devices, vol. ED-32, pp. 2197-2205, 1985.
- [5] F. Capasso, W. T. Tsang, A. L. Hutchinson, and G. P. Williams, "Enhancement of electron impact ionization in superlattice: A new avalanche photodiode with large ionization rates ratio," Appl. Phys. Lett., vol. 40, pp. 38-40, 1982.
- [6] F. Capasso, W. T. Tsang, and G. F. Williams, "Staircase solid state photomultipliers and avalanche photodiodes with enhanced ionization rate ratio," IEEE Trans. Electron Devices, vol. ED-30, pp. 381-390, 1982.

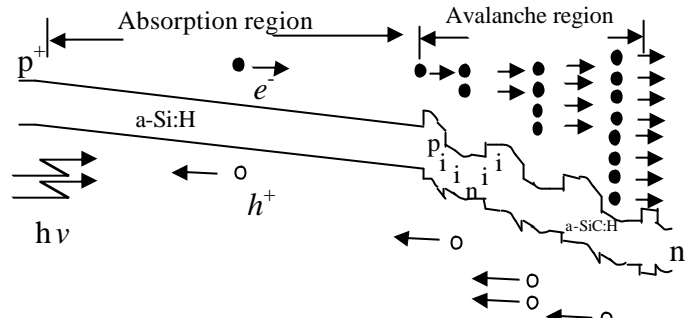


Fig.2 the energy -band diagram under reverse-bias of an amorphous SAM -DSAPD.